Frequency Selection Concurrent Sensing Technique for High Performance Touch Screens

M.G.A. Mohamed, Kyoungrok Cho, and HyungWon Kim

Abstract — *In this paper, we present frequency selection concurrent sensing (FSCS) technique for multi-touch detection of projected mutual capacitance touch screens. The proposed technique improves the signal to noise ratio (SNR) and frame scan rate of large touch screens. With proposed technique, the controller concurrently applies sine waves with different frequencies to all drive lines. It converts the outpqut signals of each sense line to frequency domain using Fast Fourier Transform (FFT), and measures the touch signal strength at the frequency corresponding to each touch position. We show that the proposed method can substantially improve the SNR by properly selecting the frequencies for the excitation signals to avoid the ambient noise. We also demonstrate that the FSCS technique can significantly increase the frame scan rate by concurrently driving all lines. Experimental results show that the proposed technique provides a frame scan rate of 128.2Hz and an SNR of 70.5dB with a large touch screen of 23 inches.*

Index Terms — Multi-Touch, Frequency Selection Concurrent Sensing, Touch Screen, Controller, Mutual Capacitance.

I. INTRODUCTION

The capacitive touch screen technology has been widely adopted for small touch screen panels (TSPs) like smart phones and tablets [1]. Recently, there is increasing demand for large TSPs to support PC monitors, medical devices and electronic whiteboards. However, for large TSPs, many performance metrics didn't reach acceptable level such as signal to noise ratio (SNR), frame scan rate and report rate [2].

Capacitive TSPs have different patterns of driving and sensing lines using thin transparent electrodes of Indium Tin Oxide (ITO) or metal mesh. The patterns on TSPs are usually designed in a way to control TSP parameters, and therefore improve the touch detection sensitivity [3].

When a human body comes close to the TSP, the value of the capacitance between electrodes changes. Therefore the touch position is determined by measuring the change in the capacitance value. There are two kinds of capacitive TSPs: self-capacitance and mutual capacitance types. In self-capacitance TSPs, the horizontal and vertical electrodes are driven together to measure the change of self-capacitance of each crossing point, which is called a cell. Self-capacitance TSPs, however, suffer from ghost point problems [1], and so are usually used for single touch. On the other hand, controllers for mutual capacitance TSPs drive only the horizontal lines, and read out the vertical lines to measure the change in mutual capacitance of each cell [1]. Therefore, mutual capacitance TSPs allow
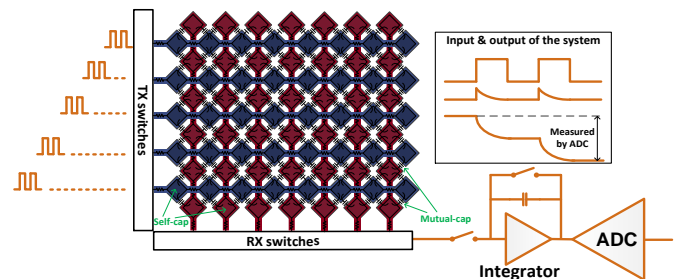
multi-touch detection, and so are more widely adopted. Most of conventional touch screen controller systems drive excitation signals onto drive (TX) lines and read out sensing (RX) lines sequentially to detect the touched points.

While the conventional touch screen controllers provide acceptable performance [4-6] for small TSPs, their speed and performance are often limited for large TSPs due to large display and power supply noise. In general, large TSPs have high parasitic resistance and capacitance values making it hard to achieve the target performance. Fig. 1 shows a conventional touch detection technique, which measures the mutual-capacitance between each TX and RX line by driving pulse signals to each TX line and integrating the output signal coming from the RX line. Hence the frame scan rate is given by the following formula:

$$Scan\ rate_{(Conv.Sch.)} = \frac{f_{drive}}{N_{integration} \times N_{tx} \times N_{rx}} \qquad (1)$$

Here, N_{tx} is the number of TX lines, N_{rx} is the number of RX lines, and f_{drive} is the frequency of TX signal. $N_{integration}$ is the number of integration steps (or the number of TX pulses per sensing cell). As indicated in Eq. (1), conventional touch screen controller systems sequentially drive each TX line and sequentially sense each RX line, resulting in unacceptably low frame scan rate for large TSPs.

Previous research has been done to improve the frame scan rate and signal to noise ratio as they are the most important issues in touch controller design [2, 7]. Mutual capacitance TSPs are highly susceptible to noise, so some research efforts have been primarily focused on noise cancelation [8-11] by manipulating differential sensing scheme. Other research efforts used either software algorithm approaches [12-14], and/or circuit-level approaches to address the noise issues. On the other hand, the target frame scan rate for small and medium size screens was easy to achieve. However, in case of large TSPs, other algorithms have been proposed to scan only the

Fig. 1. Conventional touch screen controller system used for scanning projected mutual capacitance touch screen panels.

Correspondence should be addressed to HyungWon Kim.

active part of TSP to improve the scan rate [11, 15]. Most of the previous methods, however, still suffer from limited performance due to high influence of noise.

In this paper, we propose a new touch screen controller that uses a proposed concurrent driving technique with differential sensing in order to improve frame scan rate and eliminate noise effects. This technique is manipulating Orthogonal Frequency Division Multiplexing (OFDM) and Time Division Multiplexing (TDM) [16, 17] to scan all cells on TSP.

This paper is organized as follows. Section II discusses TSP behavior and ambient noise. Section III introduces the proposed touch screen scanning technique. Section IV presents our touch screen controller architecture and Section V discusses important design issues for controller design. Experimental results are provided to demonstrate the performance in section VI. Finally conclusions are presented in section VII.
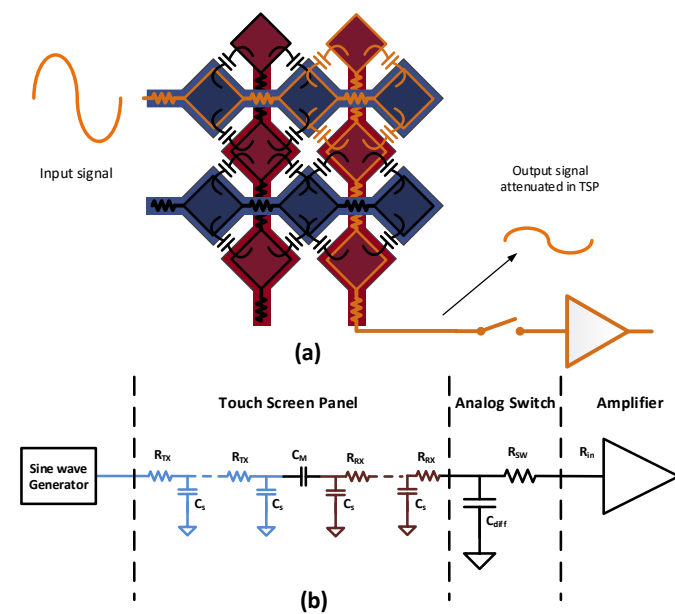

Fig. 2. Touch screen controller system modeling. (a) A part of touch screen panel driven with driving and sensing circuitry. (b) Schematic diagram used to model touch screen controller system.
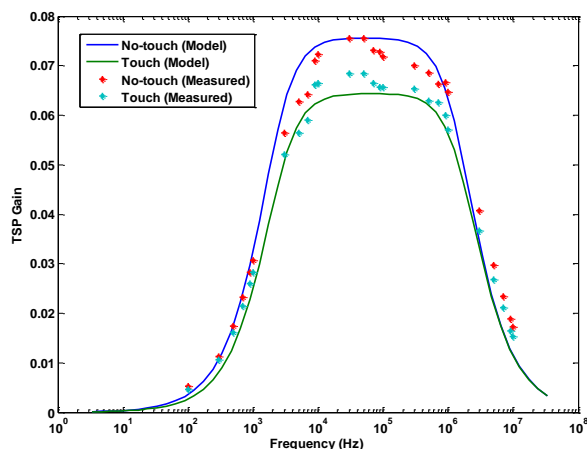

Fig. 3. Transfer function of a cell in the middle of a 23 inches commercial touch screen panel in touch and no-touch cases.

II. TOUCH SCREEN PANEL

A. Touch Screen Panel Behavior

Add-on type twolayer touch screen panels usually employ an architecture consisting of crossbar electrodes. Each cross section of such TSPs is represented by a mutual capacitor model that connects the horizontal and vertical electrodes and forms a unit cell. Each electrode is a series of transparent metal or ITO plates in order to increase the mutual capacitance value as shown in Fig. 2. Therefore one electrode can be modeled by a series of resistors and self-capacitors forming cascaded low-pass RC filter.

The transfer function of one signal path traversing through the touch screen panel has a band pass filter characteristics. Its high-pass filter cut-off frequency comes from the mutual capacitance while its low-pass filter cut-off frequency comes from the cascaded low-pass filters constructed by TX and RX lines. The resistance and self-capacitance of the electrodes limit the high cut-off frequency as they behave as a low-pass filter. Signals propagating through long paths have smaller bandwidth.

In order to measure the TSP transfer function and compare it with our model, a sine wave generator have been used to drive one TX line. By changing the input sine wave frequency, we measured the output of the TSP, and derived its transfer function. In this measurement, we used a 23-inch commercial TSP with two layers of ITO electrodes. Fig. 3 shows the measured transfer function of a cell in the center of this TSP, and it also illustrates the transfer function model by two curves. The usable pass band of the TSP ranges from 10 kHz to 1 MHz as shown in Fig. 3. It is also observed that within this range, the difference between touch and no-touch cases tends to show the largest values.

B. TSP ambient noise

It is known that mutual capacitance touch screens are sensitive to ambient noise. The values of mutual capacitances are, therefore, highly affected by noise, which is in general the primary cause of accuracy degradation. The major sources of ambient noise include florescent noise, supply noise, display noise, etc. Different noise components have different power distribution over frequency.

We measured ambient noise by reading out one RX line using oscilloscope while applying zero voltage to TX lines. Fig. 4 shows the frequency spectrum of the RX signal. Throughout repeated experiments under varying noise conditions, the noise power distribution over frequency remained same. It was observed that the ambient noise has high values in certain frequencies and low values in other frequencies. Therefore avoiding frequency bands with high noise peaks is expected to lead to higher SNR.

III. FREQUENCY SELECTION CONCURRENT SENSING TECHNIQUE

The proposed technique, Frequency Selection Concurrent Sensing (FSCS) is based on the idea of concurrently driving all the TX lines with sine waves with different frequencies. It then converts the sensed signal from each RX line to frequency domain using Fast Fourier Transform (FFT). By analyzing the

amplitude difference in every frequency component of one RX line, it identifies all the touched positions in the entire RX line at once. This technique can detect multi-touch with no ghost point problems [1].

A. The behavior of the FSCS touch detection technique

Fig. 5 illustrates the basic operation of FSCS, which simultaneously drives all sine waves with different frequencies to all TX lines, and then reads out each RX line sequentially. In other words, different TX lines are driven by sine waves with different frequencies at the same time. In this case, we can have multi-channel sensing (multiplexing) which saves time and improves scan rate. The output of an RX line is sampled by an analog to digital converter (ADC), and then fed to the FFT engine to get the frequency spectrum of the output. Next, the amplitude difference detector finds which frequency components have changes in their amplitude, and so determines whether a touch occurred. Each sine wave propagates through different TX lines and different mutual capacitors, then they are summed up through the RX line. An RX output signal is the sum of all the sine waves with different frequencies, which are attenuated while propagating through different cells.

Choosing the appropriate frequency for each line depends on the signal path. Longer paths tend to have lower "high cut-off frequency" because of increasing number of cascaded RC circuits. Therefore, we choose lower frequency signals for driving longer paths, and vice versa.

As the input signals $\left(v_i = v_0, v_1, \cdots, v_{N_{TX}-1} \right)$ are sine waves, the output signals $\left(Y_j = Y_0, Y_1, \cdots, Y_{N_{RX}-1} \right)$ are composite signals which can be described by the following equations:

$$v_i = A_i \sin(2\pi \, x(i) \, f_0 t) \qquad (2)$$

$$Y_j = \sum_{i=0}^{N_{TX}-1} B_{i,j}(t) \sin\left(2\pi \, x(i) \, f_0 t + \theta_{i,j}(t) \right) \qquad (3)$$

$$B_{i,j} = \alpha_b \, \Delta C_{m_{i,j}}(t) \qquad (4)$$

$$\theta_{i,j} = \alpha_\theta \, \Delta C_{m_{i,j}}(t) \qquad (5)$$

Here A_i and f_i are the amplitude and frequency of the i_{th} input sine wave v_i. $B_{i,j}$ and $\theta_{i,j}$ are the attenuation and phase
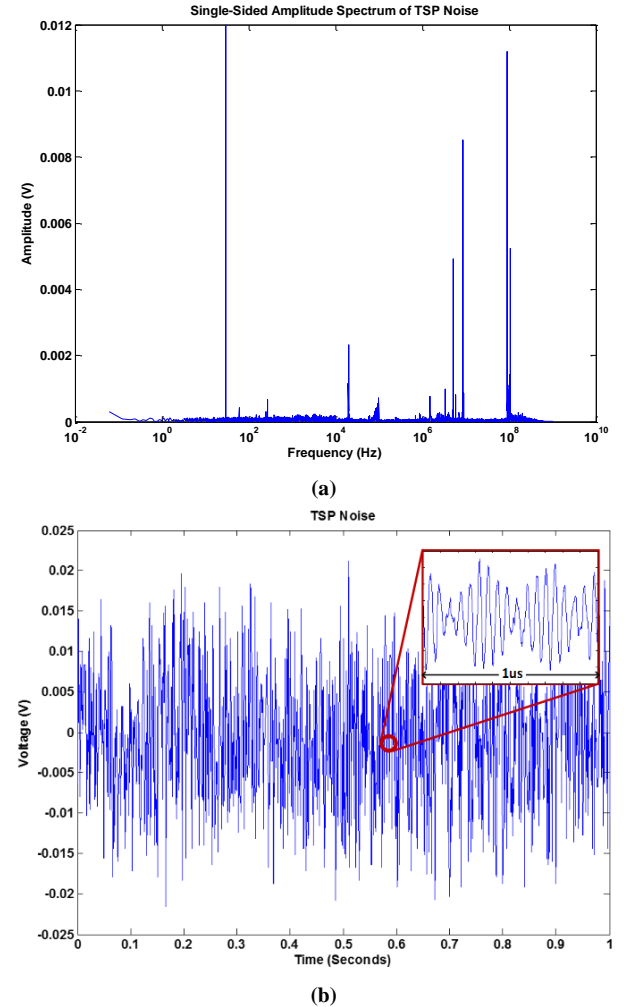

(a)

(b)

Fig. 4. Output noise of a selected RX line in a 23 inches commercial touch screen panel. (a) Frequency spectrum. (b) Time domain.
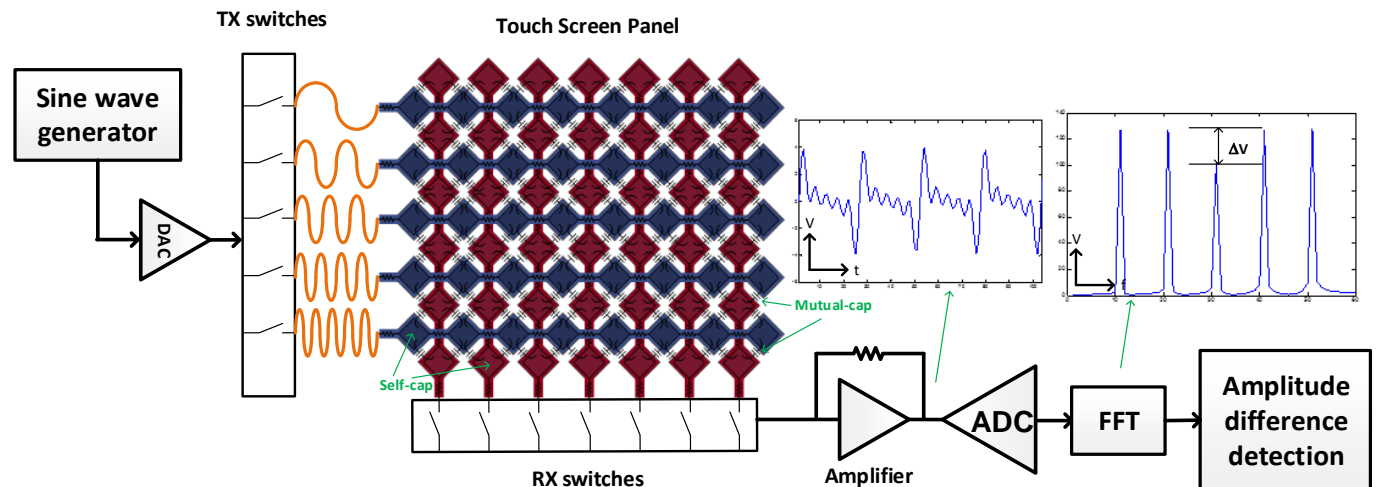

Fig. 5. Proposed Frequency Selection Concurrent Sensing FSCS technique. Sine waves with different frequencies are generated and driven to TX lines concurrently. RX lines are scanned sequentially. Output signal is amplified, then sampled and transformed to frequency domain using FFT engine. FFT output is analyzed to determine touch points.
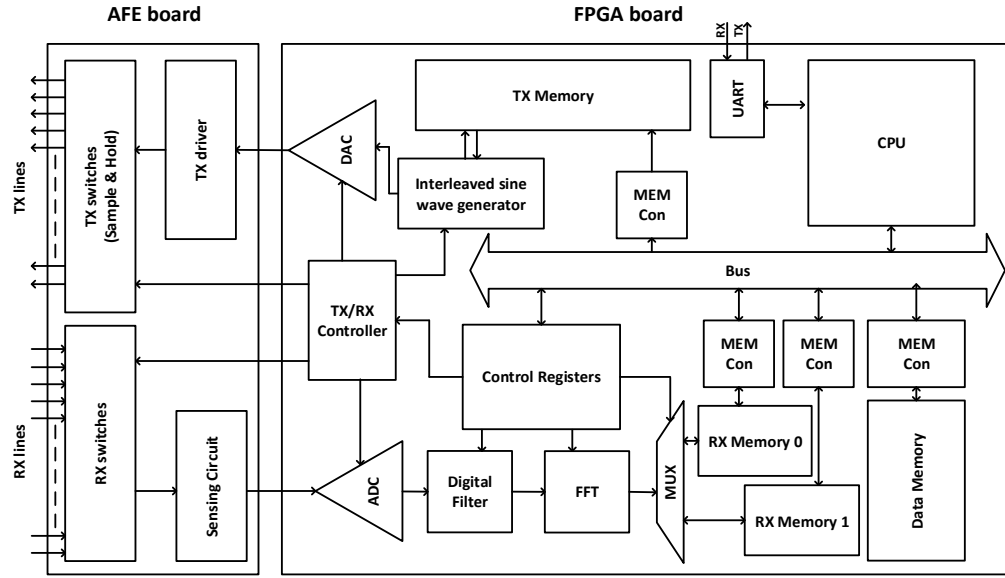
Fig. 6. Touch screen controller architecture.

shift factors imposed on the signal (v_i) when v_i passes through a touch screen path from input TX_i to output RX_j. $B_{i,j}$ and $\theta_{i,j}$ are also functions of mutual capacitance $C_{M_{i,j}}$.

As RX output signal Y_j is the sum of all sine waves applied to all TX lines with different attenuation and phase shifts, the FFT result of Y_j shows different spectral density for the frequencies f_i corresponding to the input sine waves. In this way, measuring the amplitude of the spectral density at each f_i gives the amount of change in the mutual capacitance connecting TX_i line and RX_j line.

As the noise spectrum is not equally distributed over the frequency range of the driving signals, SNR is a function of TSP transfer function and the applied frequency. Therefore different cells have different SNR values. Let $Cell_{i,j}$ be a crossing point of the i-th TX line TX_i and the j-th RX line RX_j with mutual capacitance $C_{M_{i,j}}$. $\Delta(A_i B_{i,j})$ represents the change in the output amplitude of the cell $Cell_{i,j}$. Then $SNR_{i,j}$ for $Cell_{i,j}$ can be expressed by Eq. (6).

$$SNR_{i,j} = 20\, log\left(\frac{\Delta(A_i B_{i,j})}{Noise_i}\right) \qquad (6)$$

Here, $Cell_{i,j}$ is driven by the sine wave with amplitude A_i and frequency f_i, and $Cell_{i,j}$ experiences TSP path attenuation $B_{i,j}$. $Noise_i$ is the root mean square of the noise component at frequency f_i.

B. Frequency Selection for Noise Avoidance

Overcoming ambient noise is the most challenging issue in touch screen controller design. The proposed technique utilize the flexibility of choosing noise-free frequencies for the sine waves in order to achieve higher SNR. In the case of noise condition of Fig. 4, the noise is relatively high around 10 kHz and 100 kHz. By avoiding the range of frequencies where the noise is concentrated, we can get better performance.

Most of previous approaches used differential sensing of adjacent RX lines to overcome ambient noise instead of single RX line sensing [11]. In this way ambient noise is filtered out because it generally has a common mode behavior. On the other hand, our technique provides a means to get around high noise peaks. It, therefore, can provide substantially higher SNR if it is combined with differential sensing circuitry. However we solved this issue by selecting the driving frequencies to avoid the frequency range with high noise power. For appropriate selection of the driving frequencies, noise analysis is regularly done by measuring noise spectrum at all frequencies using Fast Frequency Transform (FFT), while no driving signal applied to the TSP.

Our experiment has been done in normal operation conditions without manual injection of any particular source of noise. Hence we can consider that all ambient noise sources are included such as florescent noise, display noise, power noise, etc.

C. Differential Sensing for Noise Cancellation

Differential sensing has been used in other published techniques to cancel out common ambient noise between adjance lines. Using a differential amplifer interface, we can implement differential sensing circuitry to scan two adjacent cells, cancel the ambient noise common between the two lines and so result in a further increase in the SNR.

D. Frame scan rate improvement

The FSCS touch screen detection techniques drives all sine waves for all TX lines simultaneously. It, therefore, can significantly improve the frame scan rate of proposed touch screen controller compared to the conventional technique. As mentioned in section I, most of conventional method use square wave drive signals and integrator-based sensing circuits. They often suffer from low scan rate and low SNR. While the SNR can be improved by increasing the number of integrations, this rapidly degrades the scan rate.
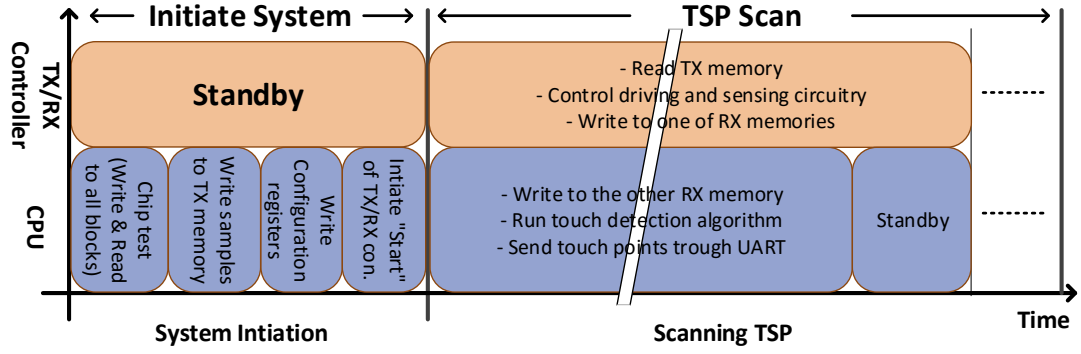
Fig. 7. Timing flow diagram for FSCS controller operation.

In the proposed technique, the scan rate is determined by the lowest frequency used to drive the TSP. We therefore, set the lowest frequency f_0 such that it satisfies the target frame scan rate, while determining the highest frequency such that it is below the allowable upper limit of the TSP's transfer function.

In the proposed method, a sensing circuit reads one RX line for one period (T) of the output signal, which is sufficient to give information about all cells on this RX line. Therefore the time required to finish scanning one frame is $N_{RX} \times T$ and the frame scan rate is given by:

$$Scan\ rate = \frac{f_0}{N_{RX}} \qquad (7)$$

Here f_0 is the lowest sine wave frequency used for driving the TSP.

IV. TOUCH SCREEN CONTROLLER

A. Controller Structure of FSCS Technique

Fig. 6 shows the architecture of the touch screen controller hardware used to run our touch detection technique. It consists of three main functions: driving a set of TX lines, sensing a set of RX lines and running detection algorithm. It has two main controllers: CPU and TX/RX controller. The CPU is connected with functional blocks through an internal system bus. The CPU and TX/RX controller communicate through a set of control registers to define operation mode. The TX/RX controller controls the TX and RX switches. While the sine wave generator generates all sine waves simultaneously, the FFT engine calculates the spectrum density of the sensed signals. The CPU reads the FFT result of sensed data from its RX memories and runs an algorithm for touch position calculation.

Fig. 7 shows the operation of FSCS controller in a timing flow diagram. TX/RX controller is the main controller that synchronizes the clock signals for all driving and sensing circuitry. CPU is responsible of writing sample values to TX memory, reading RX memories, running touch detection algorithm, and initiating TX/RX controller.

B. Sine Wave Generation

The CPU requests TSP controller to send the start signal to TX/RX controller through a set of control registers. The TX/RX controller controls sine wave generator. The sine wave generator generates memory addresses to fetch the appropriate sample data and sends it to digital to analog converter (DAC) [18]. Fig. 8(a) shows the interleaved sine wave generator block diagram. As TX/RX controller sends sampling clock to sine wave generator, the sine wave address resolver starts to resolve the sample address for each sine wave sequentially. It sends one sample data to one TX line, the next sample to the next TX line and so on. In this way all sine waves can be concurrently generated by alternating each sine wave data over all TX lines. One set of samples is being used to reduce the size of TX memory as shown in Fig. 8(b). These sample data are repeatedly used for many sine waves. However the sine wave samples generated for different TX lines are different since they form different frequencies as shown in Fig. 8(c) and (d). Eq. (8) gives the number of samples used to generate one period of sine wave with frequency $x(i)f_0$.
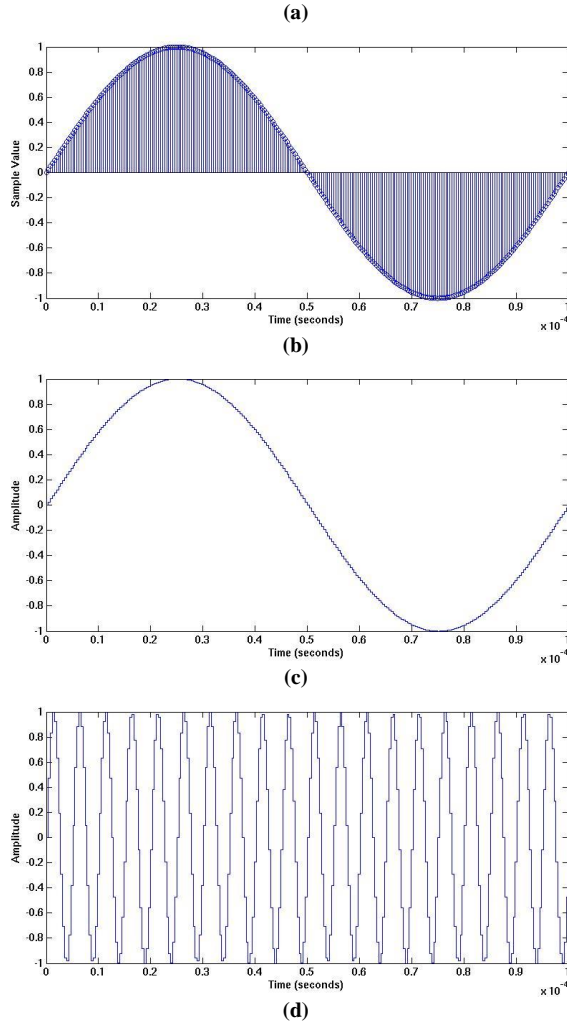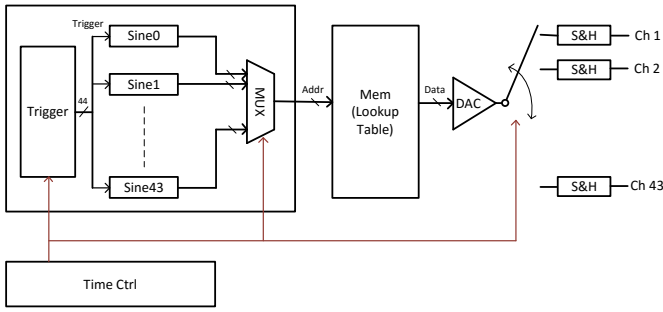
$$N_i = N_0/x(i) \qquad (8)$$

For instance, set the f_0 as 10 kHz and the number of samples stored in the memory is $N_S = N_0 = 256$. Once $x(i) = 5$ and the generated sine wave has frequency of 100 kHz, only 51.6 samples are used to generate one period of this sine wave.

The sampling frequency used to fetch data from the memory and to drive DAC is given by:

$$f_s = f_0 \times N_S \times N_{TX} \qquad (9)$$

Here N_S is the number of samples stored in the memory and used to generate the base frequency. Eq. (9) shows sampling frequency required to fetch data from the memory and feed to TX lines. For example, a touch screen with 44 TX lines use generated frequencies ranging from 10 kHz to 440 kHz. With 256 samples stored in the memory, 440 kHz sine wave uses 5.8 samples and the sampling frequency is 112.64 MHz.

Interleaved sine wave generator generates harmonics for the sine waves with high frequencies because they are generated with few number of samples. However generated harmonics affect higher frequencies that are not used in the system. It also needs smaller chip area than oscillators.

(a)

(b)

(c)

(d)

Fig. 8.   Interleaved sine wave generator. (a) Architecture. (b) Set of 256 samples used to generate sine wave signal. (c) 10kHz sine wave signal generated with 256 samples/period. (d) 200kHz sine wave signal generated with 256 samples per 20 period.

C. FFT engine

In the proposed technique, FFT is used to convert the signal into frequency domain where sinusoidal signal will be analyzed to determine touch points. The touch detection performance depends on the output SNR which is affected by the FFT resolution.

The FFT resolution is determined by the number of points (NFFT) used for FFT design and FFT maximum frequency is determined by Nyquist rate and equals half of the sampling frequency $f_s/2$. Therefore the frequencies detected by FFT

Fig. 9.   System implementation for driving 23-inches commercial touch screen panel.

TABLE I
SPECIFICATIONS SUMMARY FOR FSCS SYSTEM IMPLEMENTATION

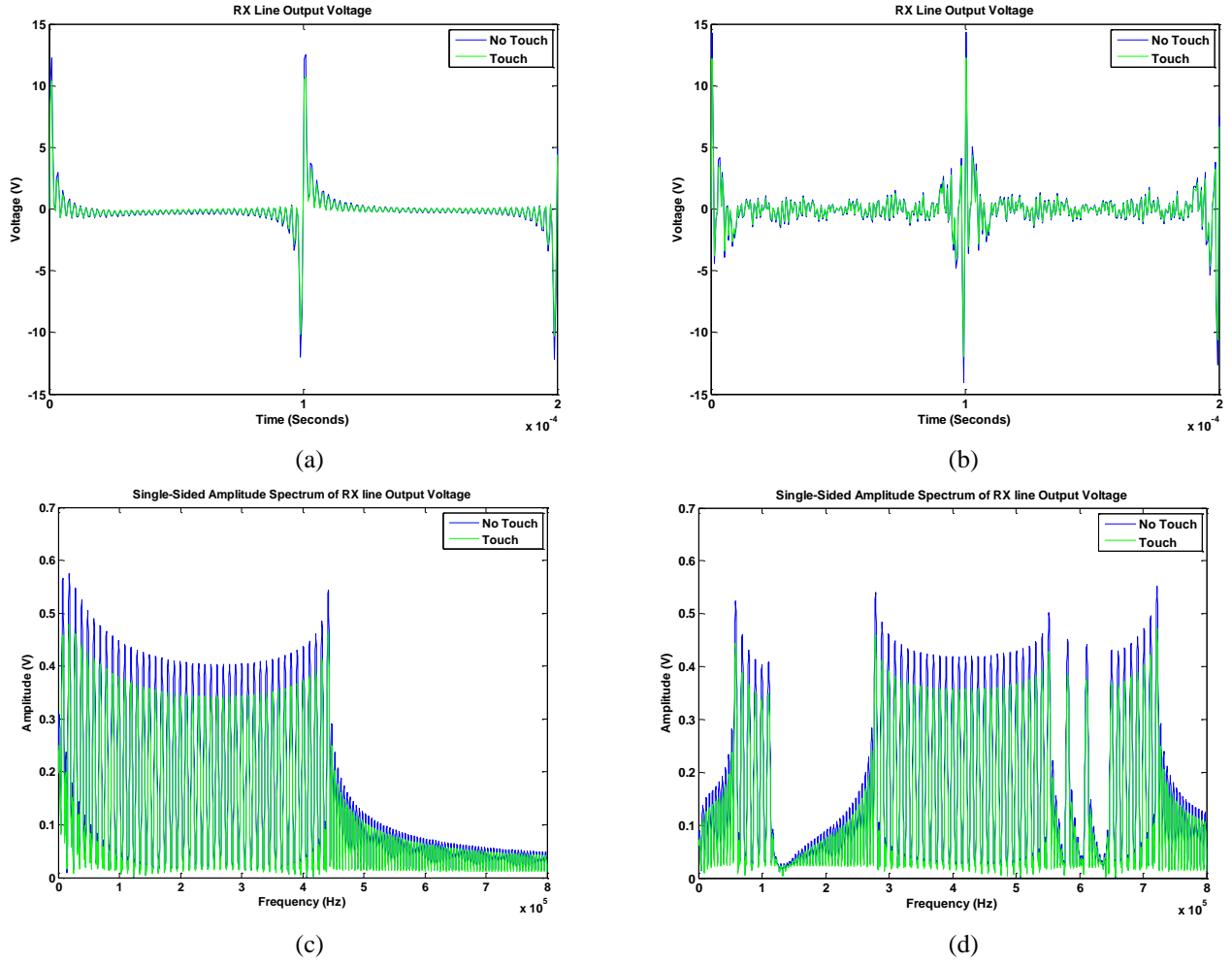|	FSCS without Noise Avoidance	FSCS with Noise Avoidance
TSP	TX lines: 44 & RX lines: 78 23-inches	
Frame scan rate	128.2 Hz	
Input voltage	5V amplitude of each sine wave	
AFE supply voltage	12V & -12V	
DAC sampling freq.	112.64 MHz	
ADC sampling freq.	2.56 MHz	
Selected (44) Frequencies	10 – 440 kHz 10 kHz freq. spacing	60 – 110 kHz 280 – 550 kHz 650 – 720 kHz 580, 610 kHz 10 kHz freq. spacing
Lowest SNR	29.3dB	52.4dB/70.5dB

engine ranges from 0 to $f_s/2$ with a step of $(f_s/2)/(NFFT/2)$. Therefore sampling frequency should also be carefully selected to high resolution of the FFT output.

Hence the shortest time taken to read one RX line is determined by the lowest frequency supplied, FFT needs a time of $(1/f_0)$, where f_0 is the lowest frequency increment between all sine waves, to calculate frequency spectrum. The detailed FFT operation and architecture of the FFT are described in [19].

Assuming the generated frequencies are integer multiples of first sine wave frequency. The lowest frequency driven to TSP has to be selected to keep FSR in acceptable range. Here is the equation employed to select the lowest frequency used for driving TSP:

$$f_0 \geq frame\ scan\ rate \times N_{RX} \qquad (10)$$

In this case, FFT needs a time of $1/f_0$ to finish scanning of every RX line, hence N_{RX}/f_0 to finish scanning of all RX lines.

(a)

(b)

(c)

(d)

Fig. 10. Simulation results for one RX line signal output. Two different input cases are presented. In (a) and (c), frequencies of input sine waves applied to TSP are multiple of 10 kHz covering the range of 10 – 440 kHz. In (b) and (d), frequencies of input sine waves are also multiple of 10 kHz, however high noise band is avoided. The frequencies of the applied sine waves cover the ranges of 60 – 110, 280 – 550, 580, 610, 650 – 720 kHz. In both cases, touch means that all cells on the selected RX line are touched, and no-touch means that all cells on the selected RX line are not touched.

V. CONTROLLER DESIGN ISSUES

There are many design aspects to consider while designing a touch screen controller based on FSCS technique. In this section, important aspects are addressed. This paper presents the key ideas of the FSCS technique using a controller architecture using one sensing circuit and one driving circuit. While this architecture minimizes the hardware requirement, the architecture can be easily expanded to multiple RX and TX circuits to proportionally increase the scan rate.

A. Sampling Frequency

Sampling frequency should be selected carefully for both driving and sensing circuitry in order to generate driving sine waves with accurate frequencies and read them again through FFT.

TX Sampling Frequency: In the driving circuit, the frequencies of generated sine waves change along with the sampling frequency of TX circuit.

As described by Sec. IV, Eq. (9) defines the sampling frequency as $(N_S \times N_{TX})$ multiples of the smallest driving sine wave frequency.

For instance, if we choose a sampling frequency of 1 MHz, a 10 kHz sine wave can be generated with 100 samples. For a TSP with 44 TX lines, 44 sine waves can be generated by choosing a sampling frequency that is 44 times higher than the single sine wave case for the single DAC architecture example.

RX Sampling Frequency: In the sensing circuit, sampling frequency should be used to precisely sense the driving frequencies. Hence the sampling frequency should be selected carefully along with the number of points of FFT.

One of the design goals of FFT is to keep its hardware cost minimum while ensuring that it covers and all the sine wave frequencies and satisfies the orthogonal property of all the frequencies. Eq. (11) expresses the minimum FFT size that satisfies this goal.

Considering FFT engine with NFFT points and sampling frequency f_s, measured frequencies f_m are given by:

$$f_m = n \frac{f_s}{2} \qquad where \ (n = 0 \sim \frac{NFFT}{2} + 1) \qquad (11)$$

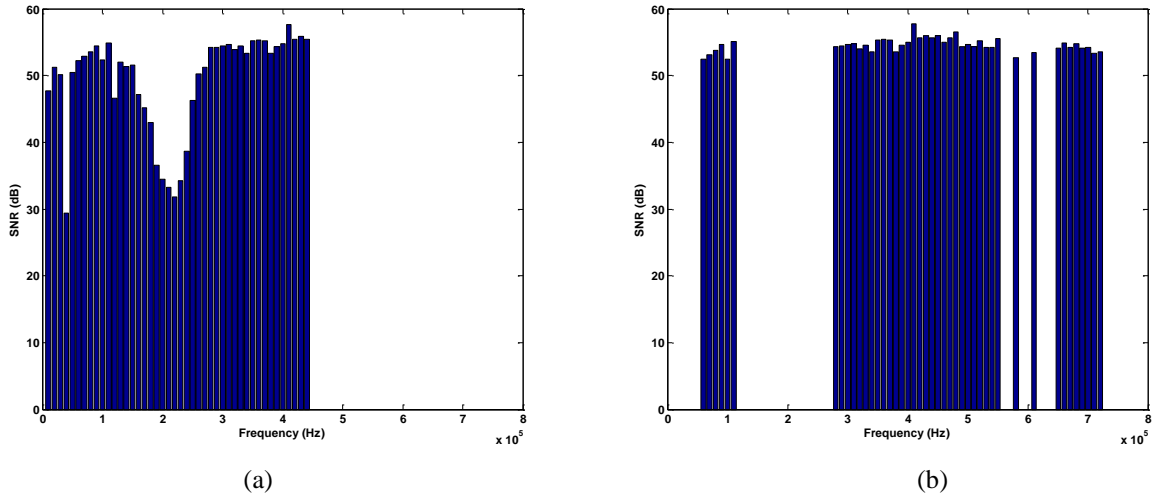(a)   (b)

Fig. 11.   Calculated SNR for different frequencies selected for driving TSP. (a) All input sine waves frequencies are multiples of 10 kHz. They range from 10 kHz to 440 kHz with 10 kHz frequency spacing. (b) Input sine waves frequencies have wider range of frequency after skipping noise band.
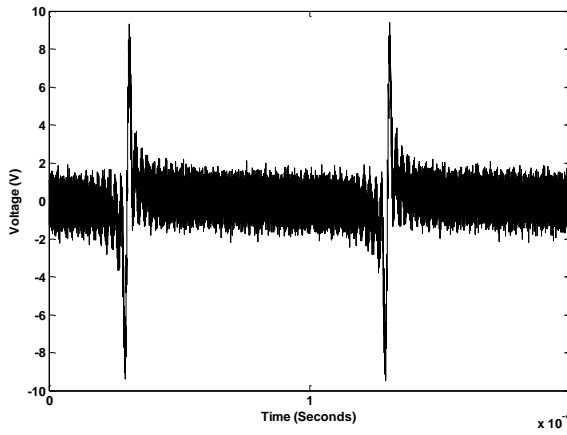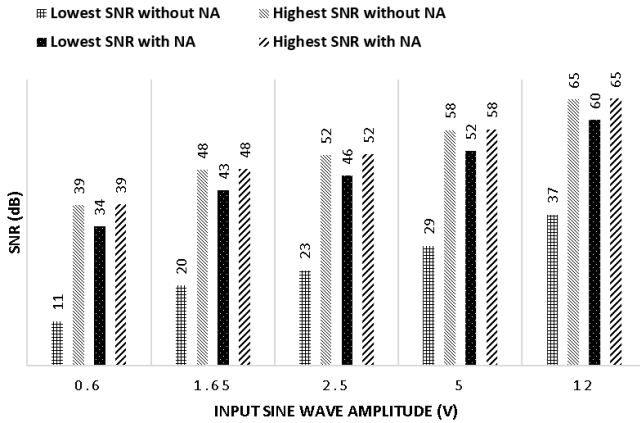

Fig. 12.   Measured RX output signal.

Fig. 13. Calculated SNR for different input sine waves amplitudes. SNR calculations are based on data extracted from a commercial 23-inches TSP.

where the number of FFT points (NFFT) should be 2^k where k is an interger.

For example, a 23-inches TSP with 44 TX lines driven by sine waves with multiples of 10 kHz (10, 20, … ,440 kHz) and FFT engine with 256 points, sampling frequency should be higher than 880 kHz to satisfy Nyquist rate. However higher

output resolution can be obtained by adjusting the sampling frequencies to match the measured frequencies f_m with input frequencies f_i.

$$f_0 = n\Delta f_m \qquad where\ (n = 1,2,3,\dots) \qquad (12)$$

Here Δf_m is the frequency gap between measured frequencies by FFT, and f_0 is the base frequency and the smallest frequency gap between input frequencies.

B.   Selected Frequency Range

Selected frequency range for input signal is determined by taking into account the following issues

TSP behavior: As shown in Fig. 3, the pass band of the TSP under test ranges from 10 kHz up to 1 MHz. Through this range the difference between touch and no-touch cases is maximum, and so the SNR. Therefore the frequencies of the input sine waves should be selected in this range. Since different TSPs usually have different pass bands, we need to select different range of frequencies for driving sine waves.

Most of TSPs exhibit their transfer function amplitude decreasing as frequency increases. To achieve higher SNR performance, therefore, our technique selects sine waves with higher frequencies for shorter paths over TSP.

Scan rate: On the other hand, frequency should be selected to give the target scan rate. Lowest frequency should be high enough in order to result in the required scan rate. In order to obtain correct FFT outputs, at least one full period of RX signal should be provided to the FFT as input. The minimum time required to finish one frame scan, therefore, is one full period of the minimum frequency sine wave.

VI.   FSCS SYSTEM PERFORMANCE

A.   System Implementation

We have implemented the proposed FSCS technique in a system hardware as shown in Fig. 9. We used a 23" commercial TSP as a test vehicle. The system implementation consists of an FPGA board for digital circuit and an analog front-end (AFE) board for analog driving and sensing circuits of Fig. 6.

Table I shows system parameters of the system

implementation. The TSP has 44 TX lines and 78 RX lines. In order to achieve the desired scan rate (> 100 Hz), the lowest frequency applied is chosen to be 10 kHz, and so the applied frequencies range from 10 kHz to 440 kHz with 10 kHz spacing. To generate sine waves of frequencies, the sampling frequency of DAC is selected to be 10 kHz x 44 x 256 = 112.64 MHz by Eq. (9).

256 samples are used to generate any sine wave in a time span of $1/f_0 = 0.1$ milliseconds. In this case, 10 kHz sine wave has 256 samples/period and 440 kHz has 5.8 samples/period.

We chose the FFT size as NFFT = 256 points to allow wide enough frequency range for flexible frequency selection. For the 256-point FFT, 256 samples are used by FFT in 0.1 milliseconds to scan frequency range of 0~1.28 MHz with a frequency resolution of 10 kHz. The frequencies that this FFT can measure, therefore, are 0, 10 kHz, 20 kHz, ….., 1,280 kHz. In the presented architecture example with one sensing circuit using only one ADC, the ADC's sampling frequency is 44 times lower than DAC frequency, and so it is 2.56 MHz. For accurate FFT result with 256 points, the ADC sampling frequency is selected to be 44 times lower than DAC frequency (2.56 MHz).

We also simulated the implemented system using a realistic model of the 23 inch 44 x 78 line touch screen panel. The TSP model is implemented by expanding the basic model of Fig. 2 to 44 TX lines and 78 RX lines. In addition, we measured the ambient noise (Fig. 4) from a real 23-inch TSP. Then we added the measured noise in order to ensure that the simulation environment can emulate the realistic operation and consequently calculate accurate SNR for the FSCS implementation.

B. Experiment results

Fig. 10 illustrates the simulation results obtained using the simulation environment described above. The experiments have been conducted using the 23-inch TSP with 44 TX lines and 78 RX lines. Fig. 10(a) and (c) show the simulation results of one RX output without applying noise avoidance (NA) technique. We applied 44 sine waves with frequencies from 10 kHz to 440 kHz. The measured noise is also applied to TSP model in order to get a close to reality simulation.

Fig 10(b) and (d) shows the simulation results with noise avoidance technique. In this experiment, we applied the measured noise, which is illustrated in Fig. 4. In case of applying noise avoidance, the proposed noise avoidance selected only input frequencies that have an SNR higher than 50 dB. The scan rate with noise avoidance case is the same as the case without noise avoidance. This follows from the fact that we used the same frequency spacing 10 kHz and the 256-point FFT has wide enough frequency range to discard many unacceptable frequencies.

Fig. 11 shows the SNR values calculated for the proposed technique with and without applying noise avoidance technique. One RX line has been read out for 100 times. The signal is converted to frequency domain using FFT in order to measure the change in the values of 44 applied sine waves to detect the touched cells.

The SNR calculation is conducted using the following equations [20]:

$$SNR = 20 \, log \left(\frac{Touch \; Strength}{Noise} \right) \tag{13}$$

$$Touch \; Strength = AVG_{touch} - AVG_{no-touch} \tag{14}$$

$$Noise = \sqrt{\frac{\sum_{n \in 100}(S_{touched}[n] - AVG_{touch})^2}{100}} \tag{15}$$

Here AVG_{touch} and $AVG_{no-touch}$ are the average of 100 values read out for the case of touch and no-touch events, respectively. $S_{touched}$ is a touched sample value.

C. Measurement results

Fig. 12 shows the signal measured from one RX line output while driving the TSP with 44 TX sine waves with 5V amplitude. The measured RX output signal is similar to the simulation result of Fig. 10 (a). The signal does not experience any clipping because the AFE board chips work with -12/12 voltage supply. However, increasing the supply voltage higher than 5V results in clipping of RX signal because the signal level exceeds 12V.

Fig. 13 shows the calculated SNR values for our system setup shown in Fig. 9 with changing input sine waves' amplitudes. Increasing input sine waves' amplitudes improves output SNR because it results in an increase for the touch strength.

Fig. 14 shows absolute values for the ADC readings for one frame data measured using the system implementation with two touch points. The z-axis in Fig. 14 gives an absolute values of ADC readings, because touched points usually have lower output values than untouched points. It can be clearly observed that the noise values are significantly smaller than the touch signals' amplitude. It is observed that the ADC output values of the lines near the edge are higher than the rest of the TSP. This effect can be explained by the following analysis:

- The TSP used for our experiments have its one side of RX lines connected to the read-out bezel traces and RX connector. This structure causes higher capacitive loading on the TSP's side connected to RX connector.

- Every cell has different signal path and the mismatch in capacitance values, the ADC output value for each cell has different value.

Therefore, the touch processing usually starts by calculating the delta value for each cell by calculating the different between the absolute ADC reading and the calculated base value. Then the touch processing algorithm continues its operation using delta values.

On the other hand, there are several factors affect the frame scan rate and SNR of a TSP controller. The number of sensing circuits affect frame scan rate. The finger position extraction algorithm also affects the frame scan rate. Some techniques apply smart methods to read out only few cells of touch screen instead of reading out all cells. However, in our proposed technique, applying sine waves concurrently to the TSP lead to a high scan rate if the sine wave frequencies are high enough. Its frequency selection method provides an additional ability of avoiding frequencies with high noise concentration, and so it can significantly improve the SNR performance.

TABLE II
COMPARISON WITH RECENT PUBLISHED WORK

	T-CE 2010 [6]	ASSCC 2010 [21]	T-CE 2011 [22]	IEEE-CAS-I 2013 [23]	ISSCC 2013 [24]	ISSCC 2014 [25]	ISSCC 2014 [8]	JSSC 2014 [4]	JS 2015 [11]	This work
Implementation	FPGA + AFE board	0.18 um	0.35 um	0.35 us	0.18 us	0.35	0.18	0.18	FPGA + AFE board	FPGA + AFE board
Size	7x9 3.5-inches	16x20	29x53 13.3-inches	27x43 10.1-inches	30x24	80x80	24x16	12x8	44x78 23-inches	44x78 23-inches
Frame scan rate (Hz)	-	65	140	120	240	322 (1-finger)	160	200	301.64 (5-fingers)	128.64
Normalized scan rate (kHz)$^{(2)}$	-	20.8	215.2	139.3	172.8	103	61.44	19.2	199.1	441.5
Scan type	All cells	All cells	All cells	All cells	All cells	Selective[1]	All cells	All cells	Selective[1]	All cells
No. of sensing circuits	1 / RX	1 / 4RX	1 / RX	1 / RX	1 / RX	1/RX + 1/TX	1 / 4RX	1 / RX	1	1
Excitation signal peak-peak	-	Up to 3.3	3.3	Up to 3.3	Up to 3.3	Up to 3.6	Up to 3.3	Up to 3.3	5	5
SNR (dB)	21.3	24	12.6	39	55	41	53	60	32/61.6	52.4/70.5
Sensing type	Single-line	Single-line	Differential	Differential	Differential	Single-line	Differential	Differential	Single-line/ Differential	Single-line/ Differential

[1] Selective scan technique refers to applying smarter algorithm to scan only affected cell, instead of reading out all cells. Developed selective scan techniques have two steps of scanning: first step is for finding out touched areas, and second step is for deeply scan of touched areas.

[2] Normalized scan rate refers to the rate of scanning one cell on the TSP.

Table II compares the performance of the proposed FSCS technique with the previous read out circuits introduced by latest published articles. It can be observed from Table II that the number of sensing circuits and supply voltage have large impact on the frame scan rate.
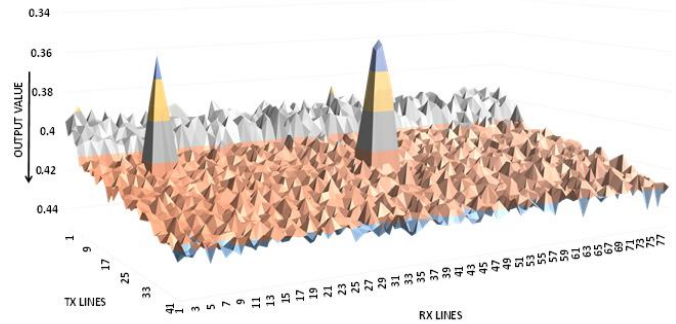
Proposed technique implementation with FPGA and analog front end board to scan a 23-inch TSP gives a frame scan rate of 128.2 MHz and SNR of 52.4 dB with single-line sensing. However SNR increases to 70.5 dB with differential sensing. On contrary, previous techniques provide lower SNR. However selective scan alogrithms [11, 15, 25] can have higher scan rate by scanning only the active part on the TSP. These technique have reduced performance with many simultaneous touch events.

VII. CONCLUSION

In this paper, we presented a new technique for multi-touch detection of projected mutual capacitance touch screen panels. The proposed technique is implemented with FPGA and analog front-end board to scan a 23-inch touch screen panel. Through the technique, sine waves with different frequencies are concurrently driven to touch screen panel and Fast Fourier Transform is used to analyze output signal. Concurrent driving enables simultaneous multiple cells scan and consequently high scan rate. This technique has high signal to noise ratio because frequencies of input signals can easily be selected to avoid high noise band. Implementation of the proposed technique gives a frame scan rate of 112.64 MHz and SNR of 52.4dB with single-line sensing and 70.5dB with differential-line sensing.

ACKNOWLEDGMENT

Fig. 14. One frame data with two touch points.

REFERENCES

[1] G. Barrett and R. Omote. (2010) Projected-Capacitive Touch Technology. *Information Display*. 16-21.

[2] A. Ng and P. H. Dietz, "The Need for Speed in Touch Systems," *SID Symposium Digest of Technical Papers,* vol. 44, pp. 547-550, 2013.

[3] J. Lee, M. T. Cole, J. C. S. Lai, and A. Nathan, "An Analysis of Electrode Patterns in Capacitive Touch Screen Panels," *Journal of Display Technology,* vol. 10, pp. 362-366, 2014.

[4] J.-E. Park, D.-H. Lim, and D.-K. Jeong, "A Reconfigurable 40-to-67 dB SNR, 50-to-6400 Hz Frame-Rate, Column-Parallel Readout IC for Capacitive Touch-Screen Panels," *IEEE Journal of Solid-State Circuits,* vol. 49, pp. 2305-2318, 2014.

[5] H.-R. Kim, Y.-K. Choi, S.-H. Byun, S.-W. Kim, K.-H. Choi, H.-Y. Ahn, *et al.*, "A mobile-display-driver IC embedding a capacitive-touch-screen controller system," in *IEEE International Solid-State Circuits Conference Digest of Technical Papers (ISSCC)*, 2010, pp. 114-115.

[6] S. Ko, H. Shin, J. Lee, H. Jang, B.-C. So, I. Yun, *et al.*, "Low noise capacitive sensor for multi-touch mobile handset's applications," in *IEEE Asian Solid State Circuits Conference (A-SSCC)*, 2010, pp. 1-4.

[7] A. Ng, J. Lepinski, D. Wigdor, S. Sanders, and P. Dietz, "Designing for low-latency direct-touch input," presented at the Proceedings of the 25th annual ACM symposium on User interface software and technology,

Cambridge, Massachusetts, USA, 2012.

[8] H. Jang, H. Shin, S. Ko, I. Yun, and K. Lee, "2D Coded-aperture-based ultra-compact capacitive touch-screen controller with 40 reconfigurable channels," in *IEEE International Solid-State Circuits Conference Digest of Technical Papers (ISSCC)*, 2014, pp. 218-219.

[9] J.-H. Yang, S.-H. Park, J.-Y. Jeon, H.-S. Kim, C.-B. Park, J.-C. Lee, *et al.*, "A High-SNR Area-Efficient Readout Circuit using a Delta-Integration Method for Capacitive Touch Screen Panels," *SID Symposium Digest of Technical Papers,* vol. 43, pp. 1570-1573, 2012.

[10] K. Lim, K.-S. Jung, C.-S. Jang, J.-S. Baek, and I.-B. Kang, "A Fast and Energy Efficient Single-Chip Touch Controller for Tablet Touch Applications," *Journal of Display Technology,* vol. 9, pp. 520-526, 2013.

[11] M. G. A. Mohamed and H. Kim, "Concurrent Driving Method with Fast Scan Rate for Large Mutual Capacitance Touch Screens," *Journal of Sensors,* vol. 2015, pp. 1-10, 2015.

[12] M. G. A. Mohamed, U. Jang, I. Seo, H. Kim, T.-W. Cho, H. K. Chang, *et al.*, "Efficient algorithm for accurate touch detection of large touch screen panels," in *Consumer Electronics (ISCE 2014), The 18th IEEE International Symposium on*, 2014, pp. 1-2.

[13] Y. Kim and A. H. Tewfik, "An efficient detection on capacitive touch screens using bandwidth expansion," in *6th International Symposium on Communications, Control and Signal Processing (ISCCSP)*, 2014, pp. 534-537.

[14] M. G. A. Mohamed, T.-W. Cho, and H. Kim, "Efficient Multi-Touch Detection Algorithm for Large Touch Screen Panels," *IEIE Transactions on Smart Processing and Computing,* vol. 3, pp. 246-250, 2014.

[15] M. G. A. Mohamed, H. Kim, and T.-W. Cho, "A Fast Sensing Method using Concurrent Driving and Sequential Sensing for Large Capacitance Touch Screens," *Journal of the Institute of Information and Electronics Engineers,* vol. 52, pp. 674-682, 2015.

[16] M. G. A. Mohamed, A. N. Ragheb, H. Hassan, and H. Kim, "OFDM and TDM Based Sensing Method for Large Projected Mutual-Capacitance Touch Screens," in *IEEE International Conference on Consumer Electronics ICCE*, Las Vegas, USA, 2016.

[17] U.-y. Jang and H. Kim, "Frequency Division Concurrent Sensing Method for High-Speed Detection of Large Touch Screens " *Journal of the Korea Institute of Information and Communication Engineering,* vol. 19, pp. 895-902, 2015.

[18] J. Kim, M. G. A. Mohamed, and H. Kim, "Design of a Frequency Division Concurrent Sine Wave Generator for an Efficient Touch Screen Controller SoC," in *19th IEEE International Symposium on Consumer Electronics*, Madrid, Spain, 2015.

[19] G. Choi;, M. G. A. Mohamed;, and H. Kim, "New FFT Design with Enhanced Scan Rate for Frequency Division Concurrent Sensing of Mutual-Capacitance Touch Screens," in *International Conference on Electronics, Information and Communication ICEIC*, Danang, Vietnam, 2016.

[20] "Buttons, Sliders and Wheels :Sensor Design Guide," ATMEL, Ed., ed. ATMEL, 2011.

[21] T.-H. Hwang, W.-H. Cui, I.-S. Yang, and O.-K. Kwon, "A highly area-efficient controller for capacitive touch screen panel systems," *IEEE Transactions on Consumer Electronics,* vol. 56, pp. 1115-1122, 2010.

[22] I.-S. Yang and O.-K. Kwon, "A touch controller using differential sensing method for on-cell capacitive touch screen panel systems," *IEEE Transactions on Consumer Electronics,* vol. 57, pp. 1027-1032, 2011.

[23] J.-H. Yang, S.-C. Jung, Y.-S. Son, S.-T. Ryu, and G.-H. Cho, "A Noise-Immune High-Speed Readout Circuit for In-Cell Touch Screen Panels," *IEEE Transactions on Circuits and Systems I: Regular Papers,* vol. 60, pp. 1800-1809, 2013.

[24] H. Shin, S. Ko, H. Jang, I. Yun, and K. Lee, "A 55dB SNR with 240Hz frame scan rate mutual capacitor 30x24 touch-screen panel read-out IC using code-division multiple sensing technique," in *IEEE International Solid-State Circuits Conference Digest of Technical Papers (ISSCC)*, 2013, pp. 388-389.

[25] N. Miura, S. Dosho, S. Takaya, D. Fujimoto, T. Kiriyama, H. Tezuka, *et al.*, "A 1mm-pitch 80x80-channel 322Hz-frame-rate touch sensor with two-step dual-mode capacitance scan," in *IEEE International Solid-State Circuits Conference Digest of Technical Papers (ISSCC)*, 2014, pp. 216-217.

Mohamed G. A. Mohamed received his M.Sc. and B.Sc. in Electronics and Communication Engineering from Minia University, Egypt, in 2006 and 2009, Ph.D. in Electronics Engineering from Chungbuk National University (CBNU), South Korea in 2016. He is currently working as a senior research engineer at Silicon Works Co., Ltd., South Korea, where he is developing touch display driver ICs for mobile and automobile solutions. Mr. Mohamed did research in various areas during his work in academia. His current research forcus covers the areas of mixed signal SoC design, data converters, low power circuits, computer human interaction, digital signal processing and embedded systems.

Kyoungrok Cho received the B.S. degree in electronic engineering from Kyoungpook National University, Daegu, Korea, in 1977 and the M.S. and Ph.D. degrees in electrical engineering from University of Tokyo, Tokyo, Japan, in 1989 and 1992, respectively. From 1979 to 1986, he was with the TV Research Center of LG Electronics, Korea. He is currently a Full Professor in the College of Electrical and Computer Engineering, Chungbuk National University, Cheongju, Korea. His research interests are in the field of high-speed and low-power circuit design, system-on-a-chip platform design for communication systems, and prospective complementary metal-oxide semiconductor image sensors, memristor-based circuits, and the design of multilayer system-on-systems technology. From 2008 to 2011, he was the Director of World Class University Program at Chungbuk National University. He is also a Director of the IC Design Education Center at Chungbuk National University. He was recipient of the IEEK Award in 2004. During 1999 and 2006, he was with Oregon State University, USA, as a Visiting Scholar. He is a member of the Institute of Electronics Engineers of Korea.

HyungWon Kim (M'95) received his B.S. and M.S. degree in Electrical Engineering from Korea Advanced Institute of Science and Technology (KAIST) in 1991 and 1993, respectively, and Ph.D. degree in Electrical Engineering and Computer Science from the University of Michigan, Ann Arbor, MI, US in 1999. In 1999, he joined Synopsys Inc., CA, US, where he developed electronic design automation software. In 2001, he joined Broadcom Corp., San Jose, CA, US, where he developed various network chips including a WiFi gateway router chip, a network processor for 3G, and 10gigabit ethernet chips. In 2005, he founded Xronet Corp., a Korea based wireless chip maker, where as a CTO and CEO, he managed the company to successfully develop and commercialize wireless baseband and RF chips and software including WiMAX chips supporting IEEE802.16e and WiFi chips supporting IEEE802.11a/b/g/n. Since 2013, he has been with Chungbuk National University,

Cheongju, South Korea, where he is an assistant professor in the department of Electronics Engineering. His current research focus covers the areas of wireless sensor networks, wireless vehicular communications, mixed signal SoC designs for low power sensors, and bio-medical sensors.